Heat and Mass Transfer 37 (2001) 397–402 © Springer-Verlag 2001

# Unsteady laminar MHD flow and heat transfer in the stagnation region of an impulsively spinning and translating sphere in the presence of buoyancy forces

**H. S. Takhar, A. J. Chamkha, G. Nath**



**Abstract** An analysis has been carried out to determine the development of momentum and heat transfer occurring in the laminar boundary layer of an incompressible viscous electrically conducting fluid in the stagnation region of a rotating sphere caused by the impulsive motion of the free stream velocity and the angular velocity of the sphere. At the same time the wall temperature is also suddenly increased. This analysis includes both short and long-time solutions. The partial differential equations governing the flow are solved numerically using an implicit finite-difference scheme. There is a smooth transition from the short-time solution to the long-time solution. The surface shear stresses in the longitudinal and rotating directions and the heat transfer are found to increase with time, magnetic field, buoyancy parameter and the rotation parameter.

## 1 Introduction

The study of flow and heat transfer on rotating bodies of revolution in a forced flow is useful in several engineering applications such as projectile motion, re-entry missile design of rotating machinery, fibre coating etc. The flow and (or) heat transfer on a rotating sphere in a uniform flow stream with its axis of rotation parallel to the free stream velocity have been studied by a number of investigators [1–5]. These studies deal with steady flows. Ece [6] has investigated the initial boundary layer flow past an impulsively started translating and spinning body of revolution. Recently, Ozturk and Ece [7] have considered the analogous heat transfer problem. The effect of buoyancy forces on the steady forced convection flow over a rotating sphere was studied by Rajasekaran and Palekar [8]. The corresponding unsteady case was considered by Hatzikonstantinou [9], where the unsteadiness was introduced by the time dependent free stream velocity.

When the unsteadiness in the flow field is caused by the impulsive motion of the body in an otherwise ambient fluid, the inviscid flow over the body is developed instantaneously. The flow within the viscous layer is developed slowly and it becomes fully developed steady-state flow after a lapse of certain time. For small time, the flow is dominated by the viscous force and the unsteady acceleration and is generally independent of the conditions far upstream and at the leading edge or at the stagnation point. For large time the flow is dominated by the viscous force, pressure gradient and convective acceleration. The influence of the conditions at the leading edge or at the stagnation point plays an important role during this phase. For small time, the mathematical problem is of the Rayleigh type and for large time it is of the Falkner–Skan type.

The boundary layer flow development on a semi-infinite flat plate due to an impulsive motion was studied by Stewartson [10, 11], Hall [12] and Watkins [13]. The corresponding problem on a wedge was investigated by Smith [14], Nanbu [15] and Williams and Rhyne [16].

In the present paper, we have studied the unsteady laminar incompressible boundary layer flow and heat transfer of an electrically conducting fluid in the forward stagnation-point region of a sphere with an applied magnetic field, where the unsteadiness is caused by the impulsive motion of the fluid and the impulsive rotation of the sphere. At the same time, the temperature of the surface of the sphere is suddenly raised. Both short-time and long-time solutions are included in the analysis. The partial differential equations governing the flow are solved numerically using an implicit finite-difference scheme [17]. The results of the particular cases are compared with those available in the literature [5–7, 18].

## 2 Problem formulation

We consider the unsteady laminar incompressible boundary layer flow of a viscous electrically conducting fluid in the vicinity of the front stagnation point of a rotating sphere with a magnetic field and a buoyancy force. Prior to the time $t = 0$, the sphere is at rest in an ambient fluid with surface temperature $T_\infty$ which is the same as that of the surrounding fluid. At time $t = 0$, an impulsive motion is imparted to the ambient fluid and the sphere is suddenly rotated with the constant angular velocity $\Omega$. At the same time the surface temperature of the sphere is suddenly raised to $T_w$ $(T_w > T_\infty)$. The flow model and the

*Received on 27 January 2000*

H. S. Takhar (✉)
Department of Engineering
Metropolitan University Manchester
Manchester M1 5GD, UK

A. J. Chamkha
Department of Mechanical Engineering
Kuwait University
Safat – 13060, Kuwait

G. Nath
Department of Mathematics
Indian Institute of Science
Bangalore – 560012, India

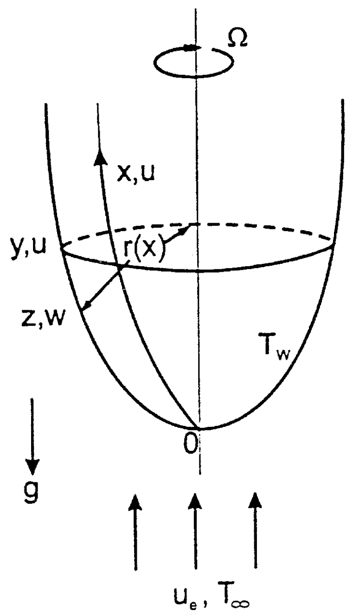


**Fig. 1.** Physical model and coordinate system

coordinate system are shown in Fig. 1. A constant magnetic field $B$ is applied in $z$ direction. It is assumed that the magnetic Reynolds number $\mathrm{Rm} = \mu_0 \sigma VL \ll 1$, where $\mu_0$ is the magnetic permeability, $\sigma$ the electrical conductivity, and $V$ and $L$ the characteristic velocity and length, respectively. Under this condition it is possible to neglect the effect of the induced magnetic field as compared to the applied magnetic field. This condition is, generally satisfied in laboratories. The wall and free stream temperatures are taken as constants. The dissipation terms, Ohmic heating and surface curvature are neglected in the vicinity of the stagnation point. The flow is assumed to be axisymmetric. The fluid has constant properties except the density changes which produce buoyancy forces. It is also assumed that the effect of the buoyancy induced streamwise pressure gradient terms on the flow and temperature fields is negligible. Under the foregoing assumptions, the boundary layer equations governing the flow can be written as [5, 7, 19, 20].

$$\frac{\partial}{\partial x}(ux) + \frac{\partial}{\partial z}(wx) = 0 \ , \tag{1}$$

$$\frac{\partial u}{\partial t} + u\frac{\partial u}{\partial x} + w\frac{\partial u}{\partial z} - \frac{v^2}{x} = u_e \frac{\mathrm{d}u_e}{\mathrm{d}x} + \nu \frac{\partial^2 u}{\partial z^2} + g\beta(T - T_\infty)\frac{x}{R} - \frac{\sigma B^2}{\rho}(u - u_e) \ , \tag{2}$$

$$\frac{\partial v}{\partial t} + u\frac{\partial v}{\partial x} + w\frac{\partial v}{\partial z} + \frac{uv}{x} = \nu \frac{\partial^2 w}{\partial z^2} - \frac{\sigma B^2}{\rho} v \ , \tag{3}$$

$$\frac{\partial T}{\partial t} + u\frac{\partial T}{\partial x} + w\frac{\partial T}{\partial z} = \frac{k}{\rho c_p}\frac{\partial^2 T}{\partial z^2} \tag{4}$$

The initial conditions are

$$u(x,z,t) = v(x,z,t) = w(x,z,t) = 0, \quad T(x,z,t) = T_\infty \quad \text{for } t < 0 \ . \tag{5}$$

The boundary conditions for $t \geq 0$ are

$$u(x,o,t) = 0, \quad v(x,o,t) = \Omega x, \quad w(x,o,t) = T_w \ , \quad u(x,\infty,t) = u_e(x), \quad v(x,\infty,t) = 0, \quad T(x,\infty,t) = T_\infty \tag{6}$$

Here $x$ is the distance along a meridian from the forward stagnation point; $y$ represents the distance in the direction of rotation; $z$ is the distance normal to the surface; $u$, $v$ and $w$ are the velocity components along $x$, $y$ and $z$ directions, respectively; $T$ is the temperature; $t$ is the time; $B$ is the magnetic field; $\rho$ and $\nu$ is the density and kinematic viscosity, respectively; $k$ is the thermal conductivity; $\Omega$ is the angular velocity of the sphere; $g$ is the acceleration due to gravity; $\beta$ is the coefficient of thermal expansion; $R$ is the radius of the sphere; $c_p$ is the specific heat at a constant pressure; and the subscripts e, w and $\infty$ denote conditions of the edge of the boundary layer, on the surface and in the free stream, respectively.

It may be remarked that certain difficulties are encountered in formulating the problem of boundary layer development due to the impulsive motion. For small time solution, we can use the scale $R = z/(\nu t)^{1/2}$, $t^* = u_e t/x$. On the other hand, for large time solution, we can use the scale defined by $\eta = z(u_e/\nu x)^{1/2}$, $t^* = u_e t/x$. If we use ($R$, $t^*$) system, only then the small time solution is obtained correctly. Similarly, if we use $(\eta, t^*)$ system, only then the small time solution fits in properly. Similarly, if we use $(\eta, t^*)$ system, only then the large time solution is found to be correct. Therefore, we have to find a scaling of the $z$-coordinate which behaves like $z/(\nu t)^{1/2}$ for small time and like $z(u_e/\nu x)^{1/2}$ for large time. Also it is convenient to choose time scale such that the region of time integration may become finite. Such transformations are given by [16].

$$\begin{aligned}
&\eta = (2a/\nu)^{1/2}\xi^{-1/2}z, \quad a > 0, \\
&\quad t^* = at, \quad \xi = 1 - \exp(-t^*), \quad u_e = ax, \\
&v_w = \Omega x, \quad u(x,z,t) = axf'(\xi,\eta), \\
&\quad v(x,z,t) = \Omega x s(\xi,\eta), \\
&w(x,z,t) = -(2a\nu)^{1/2}\xi^{1/2}f(\xi,\eta), \\
&\quad \lambda = (\Omega/a)^2, \quad \mathrm{Pr} = \mu c_p/k, \\
&T(x,z,t) = T_\infty + (T_w - T_\infty)\theta(\xi,\eta), \\
&\quad M = \sigma B^2/\rho a, \quad \alpha = \mathrm{Gr_R}/\mathrm{Re_R^2}, \\
&\mathrm{Gr_R} = g\beta(T_w - T_\infty)R^3/\nu^2, \quad \mathrm{Re_R} = aR^2/\nu \ .
\end{aligned} \tag{7}$$

We apply the above transformations to Eqs. (1)–(4) and we find that Eq. (1) is satisfied identically and Eqs. (2)–(4) reduce to

$$f''' + 4^{-1}\eta(1-\xi)f'' + \xi ff'' + 2^{-1}\xi[1 - (f')^2 + \lambda s^2] + 2^{-1}\xi M(1 - f') + 2^{-1}\xi\alpha\theta = 2^{-1}\xi(1-\xi)(\partial f'/\partial\xi) \ , \tag{8}$$

$$s'' + 4^{-1}\eta(1-\xi)s' + \xi(fs' - f's) - 2^{-1}\xi M s = 2^{-1}\xi(1-\xi)(\partial s/\partial\xi) \ , \tag{9}$$

$$\mathrm{Pr}^{-1}\theta'' + 4^{-1}\eta(1-\xi)\theta' + \xi f\theta' = 2^{-1}\xi(1-\xi)(\partial\theta/\partial\xi) \ . \tag{10}$$

The boundary conditions are

$$f(\xi,0) = f'(\xi,0) = 0, \quad s(\xi,0) = \theta(\xi,0) = 1,$$
$$f'(\xi,\infty) = 1, \quad s(\xi,\infty) = \theta(\xi,\infty) = 0 \ . \tag{11}$$

Hence $t^*$ and $\xi$ are the dimensionless time; $\eta$ is the transformed variable; $f'$ and $s$ are the dimensionless velocity components along $x$ and $y$ directions, respectively; $\theta$ is the dimensionless temperature; Pr is the Prandtl number; $a$ is the velocity gradient at the edge of the boundary layer; $Gr_R$ and $Re_R$ are the Grashof number and Reynolds number, respectively; $\alpha$ is the buoyancy parameter; and prime denotes derivative with respect to $\eta$.

Equations (8)–(10) are parabolic partial differential equations. However, for $\xi = 0(t^* = 0)$ and $\xi = 1(t^* \to \infty)$, they reduce to ordinary differential equations. For $\xi$=0, we have

$$f''' + 4^{-1}\eta f'' = 0 \ , \tag{12}$$

$$s'' + 4^{-1}\eta s' = 0 \ , \tag{13}$$

$$\mathrm{Pr}^{-1}\theta'' + 4^{-1}\eta\theta' = 0 \ , \tag{14}$$

and for $\xi = 1$, we get

$$f''' + ff'' + 2^{-1}(1 - f'^2 + \lambda s^2) + 2^{-1}M(1 - f') + 2^{-1}\alpha\theta = 0 \ , \tag{15}$$

$$s'' + fs' - f's - 2^{-1}Ms = 0 \ , \tag{16}$$

$$\mathrm{Pr}^{-1}\theta'' + f\theta' = 0 \ . \tag{17}$$

For Eqs. (12)–(17), the boundary conditions (11) can be re-written as

$$f(0) = f'(0) = 0, \quad s(0) = \theta(0) = 1,$$
$$f'(\infty) = 1, \quad s(\infty) = \theta(\infty) = 0 \ . \tag{18}$$

Equations (12)–(14) are linear equations and under the boundary conditions (18) admit closed form solution of the form

$$f = (\eta/2^{1/2})\mathrm{erf}\left(\eta/2^{3/2}\right) - (\pi)^{-1/2}[1 - \exp(-\eta^2/8)],$$
$$s = \mathrm{erfc}(\eta/2^{3/2}), \quad \theta = \mathrm{erfc}(\mathrm{Pr}^{1/2}\eta/2^{3/2}),$$
$$f' = 2^{-1/2}\mathrm{erf}(\eta/2^{3/2}), \quad s' = -(2\pi)^{-1/2}\exp(-\eta^2/8),$$
$$\theta' = -(\mathrm{Pr}/2\pi)^{1/2}\exp(-\mathrm{Pr}\eta^2/8), \quad f''(0) = (2\pi)^{-1/2} \ , \tag{19a}$$

where

$$\mathrm{erf}(\eta) = \left(2/\pi^{1/2}\right)\int_0^n \exp(-x^2)\mathrm{d}x,$$
$$\mathrm{erfc}(\eta) = 1 - \mathrm{erf}(\eta). \tag{19b}$$

It may be noted that the steady-state Eqs. (15)–(17) under the boundary conditions (18) for $M = 0$ (without magnetic field), $\alpha = 0$ (without buoyancy force) are the same as those of Lee et al. [5]. For $\lambda = 0$ (without rotation, $\alpha = 0$ (no buoyancy force) Eqs. (15) and (17) are the same as those of Sparrow et al. [19] if we apply the transformations.

$$\eta = 2^{1/2}\eta_1, \quad f(\eta) = 2^{1/2}f_1(\eta_1), \quad \theta(\eta) = \theta_1(\eta_1). \tag{20}$$

Also, Eqs. (12)–(14) under the conditions (18) governing the flow and heat transfer at the start of the motion ($\xi = 0$) are identical to the leading-order equations of Ece [6] and Ozturk and Ece [7] if we apply the transformations.

$$\eta = 2^{3/2}\eta_1, \quad f(\eta) = 2^{3/2}f_1(\eta_1), \quad s(\eta) = s_1(\eta_1), \theta_1(\eta_1) \tag{21}$$



## 3
## Methods of solution

The partial differential Eqs. (8)–(10) under conditions (11) are solved numerically by using an implicit iterative tri-diagonal finite-difference method similar to that discussed by Blottner [17]. All the first-order derivative with respect to $\xi$ is replaced by two-point backward difference formulae of the form

$$\partial A/\partial\xi = (A_{i,j} - A_{i-1,j})/\Delta\xi \ , \tag{22}$$

where $A$ is any dependent variable and $i$ and $j$ are the node locations along the $\xi$ and $\eta$ directions, respectively. First the third-order partial differential equation (8) is converted into a second order by substitutions $F = f'$. Then the second-order partial differential equations for $F$, $s$ and $\theta$ are discretized using three-point central difference formulae while all the first-order differential equations are discretized by employing the trapezoidal rule. At each line of constant $\xi$, a system of algebraic equations is obtained. With the nonlinear terms evaluated at the previous iteration, the algebraic equations are solved iteratively by using the Thomas algorithm (see Blottner [17]). The same process is repeated for next $\xi$ value and the problem is solved line by line until the desired $\xi$ value is reached. A convergence criterion based on the relative difference between the current and previous iterations is employed. When this difference reaches $10^{-5}$, the solution is assumed to have converged and the iterative process is terminated.

We have examined the effect of the grid size $\Delta\eta$ and $\Delta\xi$ and the edge of the boundary layer $\eta_\infty$ on the solution. The results presented here are independent of the grid size and $\eta_\infty$ at least up to the 4th decimal place.

## 4
## Results and discussion

We have compared our results for the surface shear stresses in the $x$ and $y$ directions ($f''(0)$, $-s'(0)$) and the surface heat transfer ($-\theta'(0)$) for $\xi = 1$ (steady-state case), $M = 0$ (no magnetic field, $\alpha = 0$ (no buoyancy force) with those of Lee et al. [5]. Also we have compared the surface sheer stress in the $x$ direction ($f''(0)$) and the surface heat transfer ($-\theta'(0)$) for $\xi = 1$, $\alpha = 0$, $\lambda = 0$ (no rotation) with the results given by Sparrow et al. [18] for the axi-symmetric case. For direct comparison we have to multiply our results by $2^{1/2}$. Our results differ at maximum by about 0.2 percent. Since both Lee et al. [5] and Sparrow et al. [18] have presented the results in tabular form, for the sake of brevity, the comparison is not shown here. Further, the surface shear stresses in the $x$ and $y$ directions ($f''(0)$, $-s'(0)$) and the surface heat transfer ($-\theta'(0)$ for $\xi = 0$ (at the start of the motion), for $M = \alpha = 0$ have been compared with those of Ece [6] and Ozturk and Ece [7]. For direct comparison, we have to multiply our results by $2^{3/2}$. Since for $\xi = 0$, the results ($f''(0), -s'(0), -\theta'(0)$) are expressed in closed form which are identical to those of [6, 7]; the comparison is not presented here.

Figures 2–4 show the effect of the magnetic parameter $M$ on the surface shear stresses in the $x$ and $y$ directions ($f''(\xi,0), -s'(\xi,0), \theta'(\xi,0)$) and on the surface heat transfer ($-\theta'(\xi,0)$) for $\alpha = \lambda = 1$, Pr = 0.7, $0 \leq \xi \leq 1$. Since $M$ is multiplied by $\xi$ (see Eqs. (8) and (9)), the surface shear stresses and the heat transfer ($f''(\xi,0), -s'(\xi,0)$) are independent of $M$ at $\xi = 0$ (at the start of the motion) and the effect of $M$ increases with $\xi$. For a given $\xi(\xi > 0), f''(\xi,0), -s'(\xi,0)$ and $-\theta'(\xi,0)$ increase with $M$ due to the enhanced Lorentz force which accelerates the fluid in the boundary layer. For $\alpha = \lambda = \xi = 1$, Pr = 0.7, $f''(\xi,0), -s'(\xi,0)$ and $-\theta'(\xi,0)$ increase, respectively, by about 53, 107 and 7% as $M$ increases from 0 to 5. The reason for weak dependence of the heat transfer at the surface ($-\theta'(\xi,0)$) on $M$ is that the magnetic field does not occur in the energy equation (see Eq. (10)) explicitly.

Similarly, for $\lambda = \alpha = 1, M = 3$, Pr = 0.7, $f''(\xi,0)$, $-s'(\xi,0)$ and $-\theta'(\xi,0)$ increase, respectively, by about 375, 255 and 65% as time $\xi$ increases from 0 to 1.

The effect of the buoyancy parameter $\alpha(\alpha \geq 0)$ on the surface shear stresses and heat transfer ($f''(\xi,0), -s'(\xi,0)$ and $-\theta'(\xi,0)$) for $M = \lambda = 1$, Pr = 0.7, $0 \leq \xi \leq 1$ is presented in Figs. 5–7. Since, like $M$, $\alpha$ is multiplied by time $\xi$, the effect of $\alpha$ does not contribute at the start of the motion ($\xi = 0$), but the effect increases with $\xi$ (see Eq. (8)). For $\xi > 0, f''(\xi,0), -s'(\xi,0)$ and $-\theta'(\xi,0)$ increase with the buoyancy parameter $\alpha(\alpha \geq 0)$ because the positive buoyancy force acts like a favorable pressure gradient which accelerates the fluid in the boundary layer. This in turn reduces the thickness of the momentum and thermal boundary layers and thus enhances the surface shear stresses and the heat transfer. For $M = \lambda = \xi = 1$, Pr = 0.7, $f''(\xi,0), -s'(\xi,0)$ and $-\theta'(\xi,0)$ increase, respectively, by about 108, 15 and 18% as $\alpha$ increases from 0 to 5. The reason for weak dependence for the surface shear stress in the $y$ direction and heat transfer ($-s'(\xi,0)$ and $-\theta'(\xi,0)$) on $\alpha$ is that the buoyancy parameter $\alpha$ does not occur explicitly in equations for $s$ and $\theta$ (see Eqs. (9) and (10)).

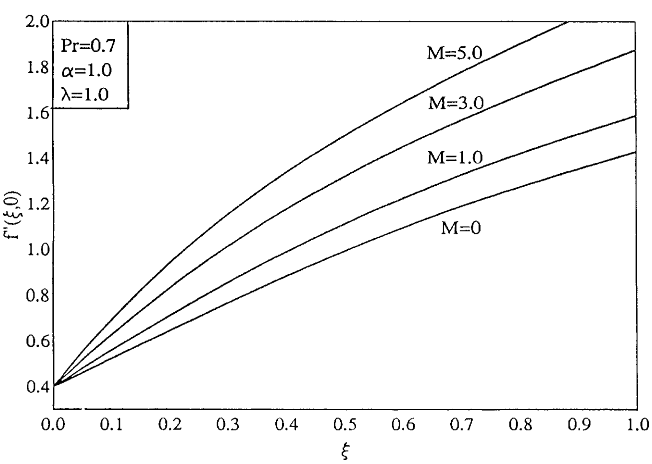


**Fig. 2.** Effect of the magnetic parameter $M$ on the surface shear stress in the $x$ direction, $f''(\xi,0)$

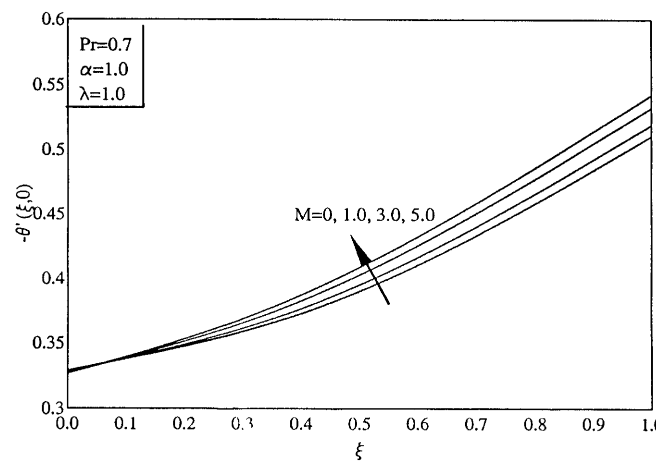


**Fig. 4.** Effect of the magnetic parameter $M$ on the surface heat transfer, $-\theta(\xi,0)$

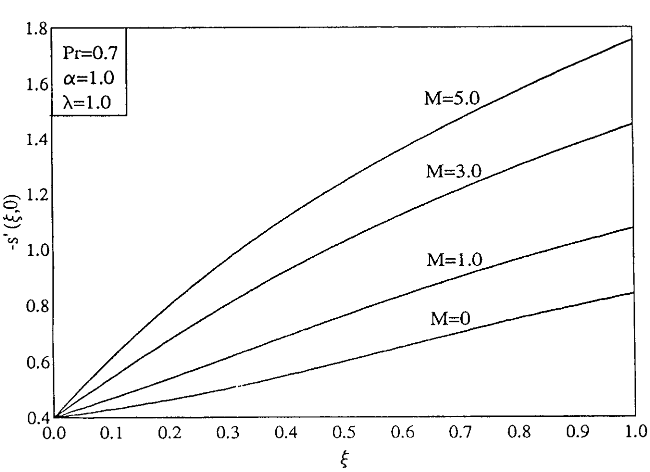


**Fig. 3.** Effect of the magnetic parameter $M$ on the surface shear stress in the $y$ direction, $-s'(\xi,0)$

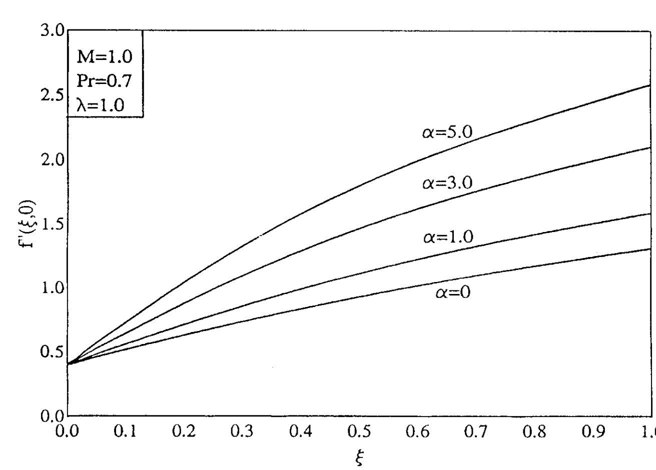


**Fig. 5.** Effect of the buoyancy parameter $\alpha$ on the surface shear stress in the $x$ directions, $f''(\xi,0)$

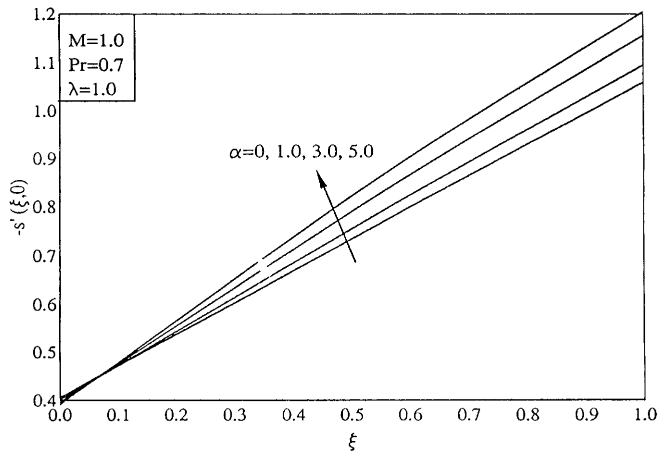


**Fig. 6.** Effect of buoyancy parameter $\alpha$ on the surface shear stress in the $y$ direction, $-s'(\xi,0)$

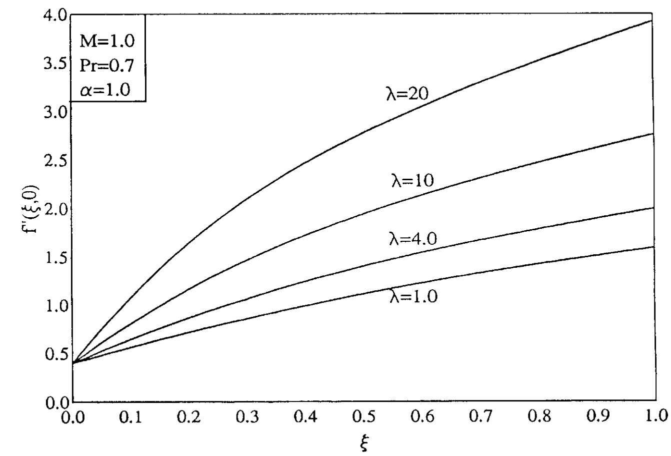


**Fig. 8.** Effect of the rotation parameter $\lambda$ on the surface shear stress in the $x$ direction, $f''(\xi,0)$

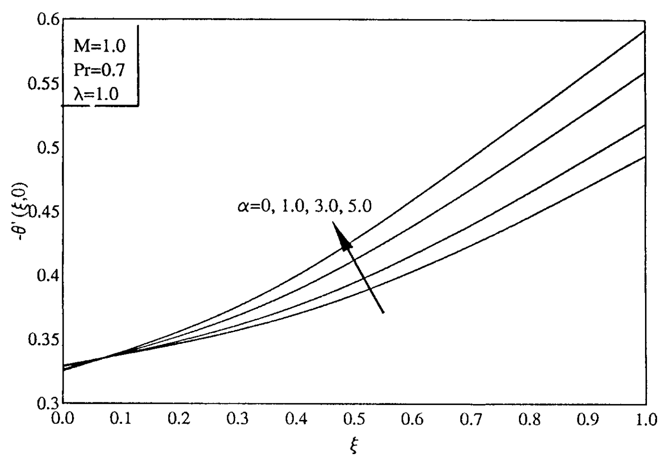


**Fig. 7.** Effect of the buoyancy parameter $\alpha$ on the surface heat transfer, $-\theta'(\xi,0)$

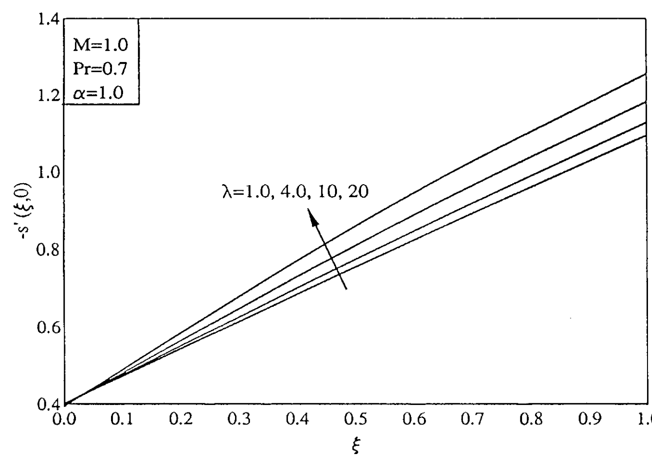


**Fig. 9.** Effect of the rotation parameter $\lambda$ on the surface shear stress in the $y$ direction, $-s'(\xi,0)$

The effect of the rotation parameter $\lambda$ on the surface shear stresses and heat transfer ($f''(\xi,0)$, $-s'(\xi,0)$ and $-\theta'(\xi,0)$) for $M=\alpha=1$, Pr = 0.7, $0 \le \xi \le 1$ is displayed in Figs. 8–10. Like $M$ and $\alpha$, the effect of $\lambda$ increases with increasing value of $\xi$. For $\xi > 0$, $f''(\xi,0)$, $-s'(\xi,0)$ and $-\theta'(\xi,0)$ increase with $\lambda$ due to the reduction of momentum and thermal boundary layers which results in an increase of the gradients of velocity and temperature at the wall. For $M=\lambda=\xi=1$, Pr = 0.7, $f''(\xi,0)$, $-s'(\xi,0)$ and $-\theta'(\xi,0)$ increase, respectively, by about 83, 7 and 10% as $\lambda$ increases from 1 to 10. Since the rotation parameter $\lambda$ does not occur explicitly in equations for $s$ and $\theta$ (see Eqs. (9) and (10)), $-s'(\xi,0)$ and $-\theta'(\xi,0)$ depend weakly on $\lambda$.

The effect of the Prandtl number Pr on the surface shear stresses and heat transfer ($f''(\xi,0)$, $-s'(\xi,0)$ and $-\theta'(\xi,0)$) for $M=\alpha=\lambda=1$, $0 \le \xi \le 1$ is shown in Figs. 11–13. Since the Prandtl number Pr occurs explicitly only in the energy equation, its effect on the surface heat transfer ($-\theta'(\xi,0)$) is very significant. However, the effect of Pr on the surface shear stresses ($f''(\xi,0)$, $-s'(\xi,0)$) is comparatively small. For $M=\alpha=\lambda=\xi=1$, $-\theta'(\xi,0)$ increases by about 201% as Pr increases from 0.7 to 15, whereas

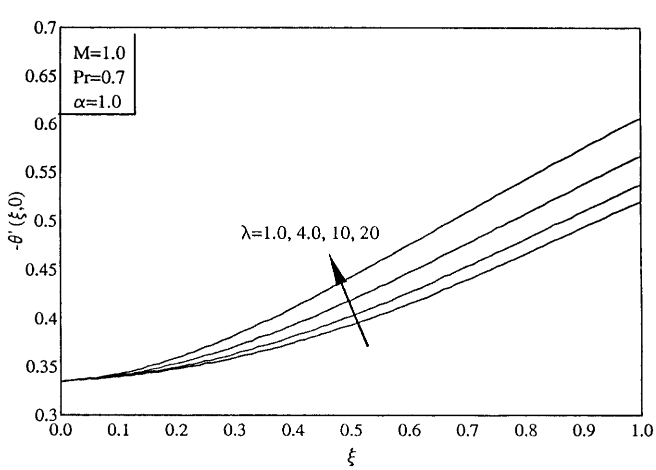


**Fig. 10.** Effect of the rotation parameter $\lambda$ on the surface heat transfer, $-\theta(\xi,0)$

($f''(\xi,0)$, $-s'(\xi,0)$) decreases by about 9 and 3%, respectively. The reason for the increase in the surface heat transfer ($-\theta'(\xi,0)$) due to the increase in the Prandtl number is that the thermal boundary layer becomes thinner with increasing Pr, whereas the momentum boundary layers become slightly thicker because higher Pr implies more viscous fluid.

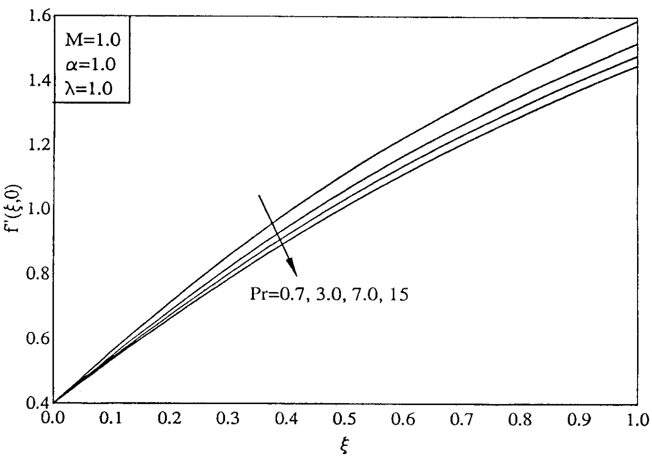


**Fig. 11.** Effect of the Prandtl number Pr on the surface shear stress in the $x$ direction, $f''(\xi, 0)$

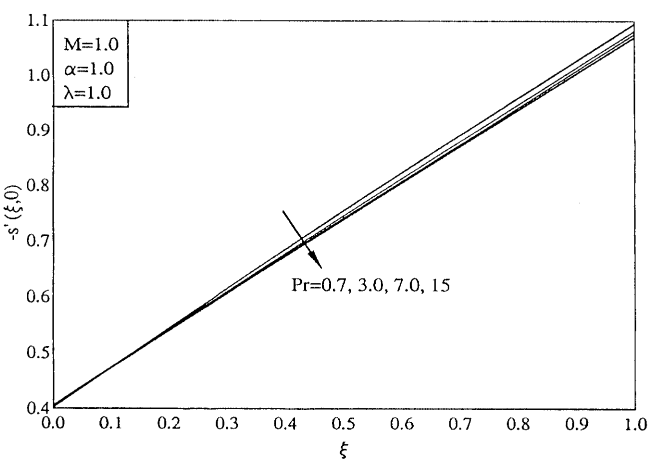


**Fig. 12.** Effect of the Prandtl number Pr on the surface shear stress in the $y$ direction, $-s'(\xi, 0)$

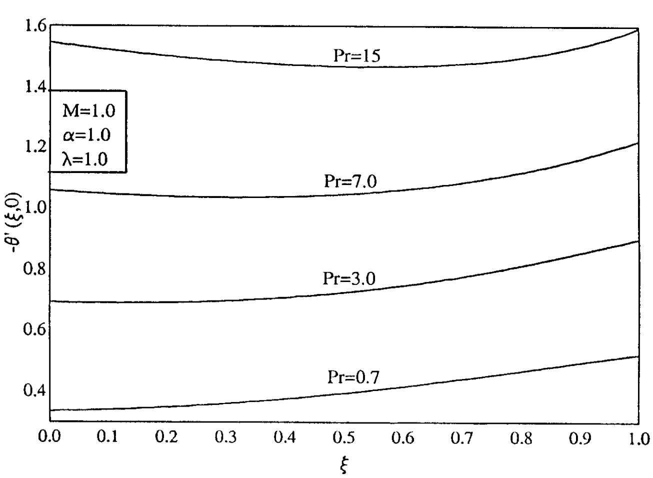


**Fig. 13.** Effect of the Prandtl number Pr on the surface heat transfer, $-\theta'(\xi, 0)$



## 5 Conclusions

The surface shear stresses in the $x$ and $y$ directions and the surface heat transfer increase with the magnetic field, buoyancy force, rotation parameter and time. There is a smooth transition from the short-time solution to the large-time solution. The surface heat transfer increases with the Prandtl number but the surface shear stresses in the $x$ and $y$ directions decrease. The surface shear stress in the $x$ direction is strongly influenced by the magnetic field, buoyancy force, rotation parameter and time. The surface heat transfer is found to be strongly dependent on the Prandtl number, but it is weakly dependent on the magnetic field, buoyancy force and rotation parameter.

## References


1. **Hoskin NE** (1955) The laminar boundary layer on a rotating sphere. In Jahre Grenzschichfforschung, pp 127–131. Friedr Vreuagel Sohn, Braunschweig
2. **Sickmann I** (1962) The calculation of the thermal laminar boundary layer on rotating sphere. ZAMP 13: 468–482
3. **Chao BT; Greif R** (1974) Laminar forced convection over rotating bodies. J Heat Transfer 96: 463–466
4. **Chao BT** (1977) An analysis of forced convection over non-isothermal surfaces via universal functions. Recent Advances in Engineering Science. In: Proceedings of the 14th Annual Meeting of the Society of Engineering Science, Leigh University, pp. 471–283
5. **Lee MH; Jang DR; Dewitt KJ** (1978) Laminar boundary layer heat transfer over rotating bodies in forced flow. J Heat Transfer 100: 496–502
6. **Ece MC** (1992) The initial boundary layer flow past a translating and spinning rotational symmetric body. J Eng Math 26: 415–428
7. **Ozturk A; Ece MC** (1995) Unsteady forced convection heat transfer from a translating and spinning body. J Energy Resources Technology (Trans ASME) 117: 318–323
8. **Rajasekaran R; Palekar MG** (1985) Mixed convection about a rotating sphere. Int J Heat Mass Transfer 28: 959–965
9. **Hatzikonstantinou H** (1990) Effects of mixed convection and viscous dissipation on heat transfer about a porous rotating sphere. ZAMM 70: 457–464
10. **Stewartson K** (1951) On the impulsive motion of a flat plate in a viscous fluid. Part I. Quart J Mech Appl Math 4: 183–198
11. **Stewartson K** (1973) On the impulsive motion of a flat plate in a viscous fluid. Part II. Quart J Mech Appl Math 26: 143–152
12. **Hall MG** (1969) The boundary layer over an impulsively started flat plate. Proc Roy Soc 310A: 401–414
13. **Watkins CA** (1975) Heat transfer in the boundary layer over an impulsively started flat plate. J Heat Transfer 97: 482–484
14. **Smith SA** (1967) The impulsive motion of a wedge in a viscous fluid. ZAMP 18: 508–522
15. **Nanbu K** (1971) Unsteady Falkner-Skan flow. ZAMP 22: 1167–1172
16. **Williams JC; Rhyne TH** (1980) Boundary layer development on a wedge impulsively set into motion. SIAM J Appl Math 38: 215–224
17. **Blottner F** (1970) Finite-difference method of solution of the boundary layer equations. AIAA J 8: 193–205
18. **Sparrow EM; Eckert ERG; Minokowycz WJ** (1962) Transpiration cooling in a magnetohydrodynamic stagnation-point flow. Appl Sci Res 11A: 125–147
19. **Eringen AC; Mougin GA** (1990) Electrodynamics of Continua, vol. 2, Springer Verlag
20. **Bush WB** (1962) The stagnation-point boundary-layer in the presence of an applied magnetic field. J Aerospace Science 28: 610–611